

Modeling the weight and length changes of the concrete exposed to sulfate using artificial neural network

Modelización de los cambios de peso y longitud del concreto expuesto al sulfato mediante red neural artificial

Veysel Akyuncu (Main Author)

Namik Kemal University, Department of Civil Engineering
Tekirdag (Turkey)
veyselak@hotmail.com

Mucteba Uysal (Corresponding Author)

Istanbul University Cerrahpasa, Department of Civil Engineering
Istanbul (Turkey)
mucteba.uysal@istanbul.edu.tr

Harun Tanyildizi

Firat University, Department of Civil Engineering
Elazig (Turkey)
htanyildizi@firat.edu.tr

Mansur Sumer

Sakarya University, Department of Civil Engineering
Sakarya (Turkey)
msumer@sakarya.edu.tr

Manuscript Code: 896

Date of Acceptance/Reception: 28.06.2018/11.04.2017

DOI: 10.7764/RDLC.17.3.337

Abstract

This paper presents the modeling of an experimental investigation carried out to evaluate some mechanical and durability properties of concrete mixtures in which cement was partially replaced with Class C and Class F fly ash. A total of 39 mixtures with different mix designs were prepared. After compressive strength testing, the mixtures containing Class F and Class C fly ashes which had similar compressive strength values to control mixtures at 28 d for each series were used for sulfate resistance tests. The degree of sulfate attack was evaluated using expansion and weight loss. The test results indicated that Class C fly ash showed higher compressive strength than Class F fly ash. Moreover, the addition of fly ash significantly increased the resistance to sulfate attack when each amount of fly ash addition regardless of fly ash types was employed. In this paper, the Artificial Neural Network (ANNs) techniques were used to model the relative change in the weight and length of the concrete exposed to sulfate. The best algorithm for length changes of concrete exposed to sulfate is BFGS quasi-Newton backpropagation algorithm while the best algorithm for weight changes of concrete exposed to sulfate is the Levenberg-Marquardt backpropagation algorithm.

Key words: Class F fly ash, Class C fly ash, the weight change, the length change, sulfate resistance.

Resumen

Este artículo presenta el modelamiento de una investigación experimental llevada a cabo para evaluar algunas propiedades mecánicas y de durabilidad de mezclas de concreto en las cuales el cemento fue parcialmente reemplazado por cenizas volantes Clase C y Clase F. Se prepararon un total de 39 mezclas con diferentes diseños de mezclas. Después de la prueba de resistencia a la compresión, las mezclas que contenían cenizas volantes de Clase F y Clase C que tenían valores similares de resistencia a la compresión para controlar las mezclas en 28 d para cada serie fueron usadas en las pruebas de resistencia a los sulfatos. El grado de ataque de sulfato se evaluó mediante la expansión y la pérdida de peso. Los resultados de la prueba indicaron que la ceniza volante de clase C mostró una resistencia a la compresión mayor que de la ceniza volante de clase F. Además, la adición de cenizas volantes aumentó significativamente la resistencia al ataque de sulfatos cuando se empleó cada cantidad de adición de cenizas volantes, independientemente de los tipos de cenizas volantes. En este trabajo, las técnicas de la Red Neural Artificial (RNA) se usaron para modelar el cambio relativo en el peso y la longitud del concreto expuesto al sulfato. El mejor algoritmo para los cambios de longitud del concreto expuesto al sulfato es el algoritmo de retro propagación de BFGS quasi-Newton, mientras que el mejor algoritmo para los cambios de peso del concreto expuesto al sulfato es el algoritmo de retro propagación de Levenberg-Marquardt.

Palabras clave: Cenizas volantes clase F; Cenizas volantes clase C; El cambio de peso; El cambio de longitud; Resistencia al sulfato.

The usage of industrial by-products in concrete, both in regard to environmental pollution and the positive effect on a country's economy are beyond dispute (Topcu, & Canbaz, 2007). These waste products are often incorporated into the concrete to improve workability, mechanical and durability properties of concrete. These include fly ash, silica fume, ground granulated blast furnace slag and other calcined natural pozzolanic materials such as metakaolin (Atiş, & Karahan, 2009; Yen, Hsu, Liu, & Chen, 2007; Mohammed, & Fang, 2011; Li, & Zhao, 2003; Liu, 2010; Melo, & Carneiro, 2010). The use of these waste products in concrete is increasing because they result in lower cost of construction and improve some physical, mechanical and durability properties of concrete in aggressive environments. It has been well established that fly ash, despite its slow rate of reaction, induces significantly improved workability and higher long-term age strength by converting the calcium hydroxide into calcium silicate hydrate (C-S-H). FA is also quite effective in producing concrete with low permeability (Chung, Shon, & Kim, 2010). This definitely enhances chemical resistance by reducing the potential for ionic ingress, migration, and concentration, subsequently controlling expansion and crack associated with sulfate attack, alkali-silica reaction, and corrosion (Mehta, & Monteiro, 1993; Roy, Chye, & Northwood, 1993; Chatterji, 1995). The use of FA has been found to be beneficial in resisting the sulfate attacks into concrete because of the microstructural densification imparted by the pozzolanic reaction or secondary hydration of these materials (Jain, & Neithalath, 2010). The main useful effect of FA in concrete consists of three aspects, often called morphologic effect, pozzolanic effect, and micro aggregate effect. The morphologic effect states that there are many micro beads in FA working as "lubricating balls" when incorporated in fresh concrete; hence it benefits the fluidity. The micro aggregate effect of FA states the micro beads in FA can disperse well in concrete and combine firmly with gel produced in cement hydration, and thus promote concrete density. The pozzolanic effect is the main effect of FA, which states that the unfixed Al_2O_3 and SiO_2 in FA can be activated by $\text{Ca}(\text{OH})_2$ product of cement hydration and produce more hydrated gel. Since the gel produced from pozzolanic action can fill in the capillary in concrete, it effectively conduces to concrete strength (Cao, Sun, & Qin, 2000).

Fly ash is widely used in blended cements, and is a by-product of coal-fired electric power plants (Alonso, & Wesche, 1991). Two general classes of fly ash can be defined: low-calcium fly ash (ASTM Class F) produced by burning anthracite or bituminous coal; and high-calcium fly ash (ASTM Class C) produced by burning lignite or sub-bituminous coal (Nochaiya, Wongkeo, & Chaipanich, 2010). Class F is categorized as a normal pozzolan, a material consisting of silicate glass, modified with aluminum and iron. Class F requires $\text{Ca}(\text{OH})_2$ to form strength-developing products (pozzolanic reactivity), and therefore is used in combination with Portland cement, which produces $\text{Ca}(\text{OH})_2$ during its hydration. It lowers the heat of hydration and improves the durability when used in concrete as a cement replacement. It also contributes to concrete strength by pozzolanic and filler effects (Papadakis, 1999). The current annual worldwide production of coal ash is estimated about 700 million tonnes of which at least 70% is fly ash (Papadakis, 1999). There are 29 thermal power plants actively working in Turkey. But Class F fly ash is obtained only from Catalagzi Thermal Power Plant, FA of all other plants is Class C. As for today, the annual fly ash production is about 20 million tones which is more than the rest of all industrial wastes in Turkey (Felekoglu, 2006). Although FA is a valuable mineral admixture for blended Portland cement and concrete, only about 4% of the total available FA is used for this purpose in Turkey (Aydin, Yiğiter, & Baradan, 2005). In particular, due to the energy demand, the production rate of FA is expected to increase in the future (Felekoglu, 2006).

There have been numerous field studies on the distress caused to concrete structures generated by sulfate attack (Persson, 2003; Girardi, Vaona, & Di Maggio, 2010). Sulfate attack is one of the most aggressive environmental deteriorations that affect the long-term durability of concrete structures. The sulfate attack of concrete leads to expansion, cracking, and deterioration of many civil engineering structures exposed to sulfate environment (Al-Akhras, 2006). The sulfate attack is generally attributed to the reaction of sulfate ions with calcium hydroxide and calcium aluminate hydrate to form gypsum and ettringite. The gypsum and ettringite formed as a result of sulfate attack is significantly more voluminous (1.2 to 2.2 times) than the initial reactants. The formation of gypsum and ettringite lead to expansion, cracking, deterioration, and disruption of concrete structures (Hooton, 1993). Concrete deterioration due to MgSO_4 attack was attributed to the decalcification of C-S-H to form M-S-H, as well as the expansion caused by the formation of expansive salts (Hekal, Kishar, & Mostafa, 2002).

Tanyildizi (2016) investigated the microstructure and strength properties of lightweight mortars containing fly ash and silica subjected to sulfate attack. He found that the performance of lightweight mortars containing silica fume were higher than lightweight mortars without mineral admixture and with fly ash. Tanyildizi (2018) studied healing of mortar exposed to sulfate attack. He reported that the concrete elements exposed to the sulfate attack could be healed with the polymer containing phosphazene. Torii, & Kawamura (1994) studied the resistance of concretes containing FA in 10% MgSO_4 solution. FA appeared to significantly increase the sulfate resistance, but only above a certain content, which depended on the type of sulfate solution. Sorrentino et al. (Sorrentino, Lacroix, Gines, &

Chabanis, 1994) demonstrated by expansion and microstructural studies that concrete of moderate strength (40 MPa) was deteriorated in MgSO₄. Large quantities of secondary ettringite and gypsum and a noncohesive M-S-H were formed. In higher strength concrete (e.g., 80 MPa), the reaction resulted in some compact layers of gypsum, aragonite, and brucite, which formed a barrier to prevent further attack. Thus, expansion was negligible even after immersion in seawater for 3 years.

There were numerous studies carried out on the influence of FA in concrete mixture on mechanical and durability properties of concrete (Siddique, 2011; Malhotra, Zhang, Read, & Ryell, 2000). However, limited research work has been carried out concerning the effectiveness of Turkish Class C and Class F fly ashes in concrete and comparing their sulfate resistance properties which the mixtures containing fly ashes had similar compressive strength values to control mixtures for each series.

ANNs are increasingly applied to solve various civil engineering problems (Trtnik, Kavčič, & Turk, 2009). There have been reports on the use of ANN in the modelling of concrete compressive strength (Ni, & Wang, 2000; Lai, & Serra, 1997; Lee, 2003). Goktepe, Inan, Ramyar, & Sezer (2006) and Tanyildizi (2017) presented a neural network approach to determine sulfate expansion level of PC mortar using statistical and neural approaches. It has been pointed out that the all models exhibited relatively close performances varying within 0.91 and 0.94 in terms of R² values. Inan, Göktepe, Ramyar, & Sezer (2007) reported an ANN model to predict sulfate expansion of PC mortar using adaptive neuro-fuzzy methodology. It has been indicated that ANFIS methodology produced the most successful results and was able to predict sulfate expansion levels precisely.

The aim of this study is to construct an ANN model to predict the weight and the length change of the concretes containing Class C and Class F fly ashes subjected to sulfate environment. For this purpose, data for developing the ANN model are collected from the experiments. In the experiments, the degree of sulfate attack was evaluated by measuring the expansion of concrete prisms and weight change of concrete prisms which the specimens have been subjected to 15 % magnesium sulfate solutions for one year.

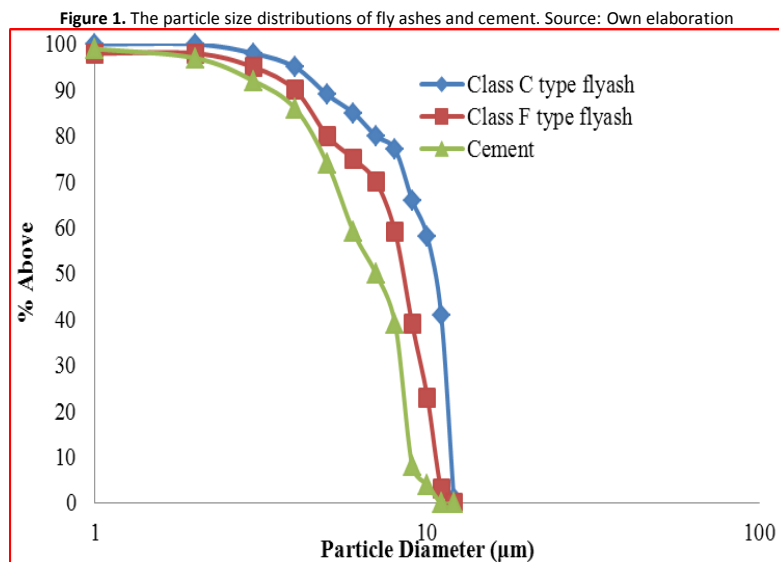
Methodology

Materials

In this study, CEM I 42.5 N Portland cement, Class C and Class F fly ashes were used as binding materials. Their chemical compositions and properties are shown in Table 1. Both Class C and Class F fly ashes were obtained from power plants in Turkey. Specific gravity of the cement used was 3.12. Initial and final setting times of the cement were 210 and 265 min, respectively. Crushed limestone aggregates with a maximum size of 16 mm were used as coarse aggregate. The specific gravity and water absorption of the aggregates were 2.71 and 0.26% and 2.69, 0.35%, respectively. A natural river sand with specific gravity of 2.61 and water absorption of 1.59 % was also employed. A uniform grading of aggregate mixture was prepared. The fineness modulus of the mixture is 4.09. Volume percentages of aggregates were kept constant in all mixtures. The particle size distributions of cement, Class C and Class F fly ashes were obtained by a laser scattering technique and are presented in Figure 1.

Table 1. Properties of Portland cement and fly ashes. Source: Own elaboration.

Component (%)	Chemical composition (%)		
	Cement	Class C fly ash	Class F fly ash
SiO ₂	20.63	46.38	58.58
Fe ₂ O ₃	3.41	8.26	6.97
Al ₂ O ₃	4.71	13.9	23.4
CaO	63.64	15.1	1.55
MgO	1.24	6.68	2.76
SO ₃	2.98	4.26	0.45
Cl ⁻	0.04	0.06	0.03
Loss Ignition	1.25	0.22	0.2
K ₂ O	0.91	2.78	4.11
Na ₂ O	0.23	2.13	0.46
Free CaO	1.1	0.15	0.1
Physical properties			
Specific Gravity	3.12	1.84	2.34
Blaine (cm ² /g)	3545	2850	3350



Mixture proportions

Three different cement dosages were used and two different ratios which 10 % and 17 % of reduced cement from the control concretes and three different ratios (depending on cement reduction ratio) of fly ash were added into the mixtures.

The workability degree of mixtures was similar to each other with a slump of 140-170 mm. The main variable in the mixtures was the cement, fly ash and the water content. The mixture proportions of the concretes are shown in Table 2 and Table 3. The raw materials of concrete were put in a forced mixer at the same time and were mixed for 3 minutes. The workability of fresh concrete including slump was measured immediately after the mixing was completed. The results are listed in Table 2 and Table 3. Slump, density and the air content of fresh concretes were obtained. The mixtures were cast into test specimens in mould by vibration. 36 series of concretes containing Class C and Class F fly ashes and 3 series of control mixtures were produced in order to investigate the compressive strength properties of concretes. After that, the mixtures containing Class F and Class C fly ashes which had similar compressive strength values to the control mixtures at age of 28 d for each series were used for sulfate resistance tests. However, the selected mixtures for sulfate resistance tests determined from two results had similar compressive strength values to the control mixtures at age of 28 d for each cement content and fly ash type. One of them was the mixture had 10% or 17% cement replacement rate (reduced cement from the control concretes) and the other one was the mixture had fly ash was added and this situation caused an increase in binder content (depending on cement reduction ratio).

Table 2. Mix proportioning of Class F type fly ash additive concretes. Source: Own elaboration.

Mix. No	Concrete Type	Class F fly ash				Water (kg)	Air Content (%)	Slump (cm)
		Cement (kg/m ³)	Remove (%)	Fly Ash (kg/m ³)	Added (%)			
M1	C260F0 (%0K0)	260	-	-	-	199	2.0	15.5
M2C	C234F26 (%10K1)	234	10	26	10.0	197	2.2	14.0
M3C	C234F39 (%10K1,5)	234	10	39	15.0	195	2.1	16.0
M4C	C234F52 (%10K2)	234	10	52	20.0	196	1.9	15.5
M5C	C216F44 (%17K1)	216	17	44	17.0	196	2.4	15.5
M6C	C216F66 (%17K1,5)	216	17	66	25.5	196	1.7	14.0
M7C	C216F88 (%17K2)	216	17	88	34.0	197	2.0	14.0
M8	C320F0 (%0K0)	320	-	-	-	205	2.3	15.5
M9C	C288F32 (%10K1)	288	10	32	10.0	186	1.6	15.5
M10C	C288F48 (%10K1,5)	288	10	48	15.0	192	1.6	15.0
M11C	C288F64 (%10K2)	288	10	64	20.0	201	1.8	14.5
M12C	C266F54 (%17K1)	266	17	54	17.0	196	1.9	14.5
M13C	C266F81 (%17K1,5)	266	17	81	25.5	201	2.1	16.0
M14C	C266F108 (%17K2)	266	17	108	34.0	203	2.0	16.0
M15	C400F0 (%0K0)	400	-	-	-	172	3.0	15.0
M16C	C360F40 (%10K1)	360	10	40	10.0	160	2.5	17.0

M17C	C360F60 (%10K1,5)	360	10	60	15.0	162	2.7	17.0
M18C	C360F80 (%10K2)	360	10	80	20.0	170	2.2	17.0
M19C	C332F68 (%17K1)	332	17	68	17.0	165	2.4	16.0
M20C	C332F102(%17K1,5)	332	17	102	25.5	164	2.4	17.0
M21C	C332F136 (%17K2)	332	17	136	34.0	180	3.0	15.5

Table 3. Mix proportioning of Class C type fly ash additive concretes. Source: Own elaboration.

Mix. No	Concrete Type	Class C fly ash				Water (kg)	Air Content (%)	Slump (cm)
		Cement (kg/m ³)	Remove (%)	Fly Ash (kg/m ³)	Added (%)			
M1	C260C0 (%0K0)	260	-	-	-	199	2.0	15.5
M2F	C234C26 (%10K1)	234	10	26	10.0	180	2.4	14.5
M3F	C234C39 (%10K1,5)	234	10	39	15.0	188	2.0	14.5
M4F	C234C52 (%10K2)	234	10	52	20.0	187	2.1	15.5
M5F	C216C44 (%17K1)	216	17	44	17.0	188	2.2	14.0
M6F	C216C66 (%17K1,5)	216	17	66	25.5	188	1.9	15.0
M7F	C216C88 (%17K2)	216	17	88	34.0	177	2.0	15.0
M8	C320C0 (%0K0)	320	-	-	-	205	2.3	15.5
M9F	C288C32 (%10K1)	288	10	32	10.0	194	1.8	15.5
M10F	C288C48 (%10K1,5)	288	10	48	15.0	192	2.2	16.5
M11F	C288C64 (%10K2)	288	10	64	20.0	182	1.8	15.0
M12F	C266C54 (%17K1)	266	17	54	17.0	185	1.9	14.5
M13F	C266C81 (%17K1,5)	266	17	81	25.5	187	2.1	17.0
M14F	C266C108 (%17K2)	266	17	108	34.0	193	2.0	17.0
M15	C400C0 (%0K0)	400	-	-	-	172	3.0	15.0
M16F	C360C40 (%10K1)	360	10	40	10.0	168	2.5	16.0
M17F	C360C60 (%10K1,5)	360	10	60	15.0	175	2.3	15.0
M18F	C360C80 (%10K2)	360	10	80	20.0	166	2.2	15.5
M19F	C332C68 (%17K1)	332	17	68	17.0	161	2.4	16.0
M20F	C332C102(%17K1,5)	332	17	102	25.5	174	2.4	14.0
M21F	C332C136 (%17K2)	332	17	136	34.0	161	3.0	17.0

Casting, testing and curing

Compressive strength test was made on 150 mm cube specimens. All specimens were demoulded in a controlled chamber at 20 ± 2 °C after 1 d of casting, and cured in lime-saturated water at 20 °C and 65% RH. Compressive strength test was performed at 28 and 90 d. Specimens of concrete with dimensions of 70x70x280 mm were used for sulfate resistance tests. The average of test results was adopted from three identical samples, for all the results. For sulfate resistance tests, the specimens were left in the mould for 24 h and then they were water cured for 28 d. After the 28 d initial curing, half of the specimens were placed in a solution of 15 % magnesium sulfate, and the rest of the specimens were placed in tap water in order to investigate the influence of the sulfate attack on the samples. The sulfate exposure testing procedure was conducted by immersing concrete specimens after the specified initial curing in a water tank containing 15 % magnesium sulfate solution at 23 ± 2 °C according to ASTM C1012-04 standard (ASTM C 1012, 2002). Sulfate solutions used for the immersion tests were renewed every 4 weeks to minimize the increase in pH due to the leaching of OH⁻ ions from the concrete specimens. Sulfate concentrations were kept relatively high to accelerate deterioration and also in order to compensate for small variations in concentration during the tests. A propeller was placed in the basin in order to secure a good circulation of the solution around the specimens. Before placing the prism specimens in the MgSO₄ solution, their lengths were measured using a high-accuracy digital length comparator. Expansion data are presented as differences between the length changes observed in magnesium sulfate solution and those in tap water. Weight change is also presented as differences between the weight changes observed in magnesium sulfate solution and those in tap water. Every month, the length and weight of each sample were measured at about 20 °C. Their weights were recorded, after surface-drying the samples with a cloth, using a technical balance with a sensitivity of 0.001 g. Their length was measured with a digital comparator with a precision of 0.001 mm.

Compressive strength

Table 4 presents the variation of compressive strength with age for various fly ash percentages of all 39 mixtures at ages of 28 d and 90 d, respectively. The test results show that the use of Class C fly ash improves the workability of concretes slightly and reduces the water requirement of the concretes when compared to Class F fly ash. Because, Class C fly ash particles had spherical shape. At age of 28 d, the compressive strength of Class C fly ash additive concretes including different amounts of fly ash can be seen to be generally higher than that of control concretes. This is especially evident in the C266C108 and C288C48 mixtures, where compressive strength reached 51.2 and 50.9 MPa, respectively and those mixtures had higher values than that of the control mixture (47.8 MPa). Moreover, the long term strength as detected at age of 90 d, the compressive strength development of Class C fly ash additive mixtures was also found to have higher strength values than the control mixtures. In the C266C108 cubic mixture compressive strength reached 59.8 MPa significantly higher than that of the control mixture, 54.9 MPa. For Class F fly ash, fly ash additive concrete mixtures including different amounts of Class F fly ash exhibited generally lower compressive strength than that of the control concretes at ages of 28 d and 90 d. The compressive strengths of the Class F fly ash mixtures decreased when the amount of fly ash was increased. From the test results, it can be seen that the use of Class C fly ash instead of Class F with the same cement dosage and fly ash percentage generally caused to higher compressive strength. As Class C fly ash, contains higher calcium amount, the compressive strength results are higher in early ages compared to Class F fly ash. 10% cement reduction by adding Class C fly ash improves compressive strength and this improvement increases with fly ash percentage. When cement is reduced by 17%, Class C and Class F fly ash additive specimens show similar behavior; compressive strength decreases with decreasing of the cement dosage and increases with adding fly ash when cement dosage is constant. Generally, the addition of Class C fly ash increased compressive strength of concrete mixtures. The slight improvement of the compressive strength obtained probably due to pozzolanic reaction. Since fly ash is a pozzolanic, the addition of fly ash should also increase concrete strength through the pozzolanic reaction. Fly ash is pozzolanic, meaning it reacts with calcium hydroxide and water to form compound with cementing properties. The two products of cement hydration are calcium silicate hydrate (C–S–H) and calcium hydroxide (CH), and of the two products, C–S–H is the major contributor to concrete strength. Supplementary cementitious materials such as fly ash contains amorphous silica (S) which reacts with calcium hydroxide (CH) to form additional C–S–H thereby improving strength (Hale, Freyne, Bush Jr, & Russell, 2008).

Table 4. Compressive strength test results of the concretes containing Class C and Class F fly ashes. Source: Own elaboration.

Class C fly ash in concrete				Class F fly ash in concrete			
Mix. No	Concrete Type	Compressive Strength (N/mm ²) 28 d	Compressive Strength (N/mm ²) 90 d	Mix. No	Concrete Type	Compressive Strength (N/mm ²) 28 d	Compressive Strength (N/mm ²) 90 d
M1	<u>C260</u>	40.20	46.20	M1	<u>C260</u>	40.20	46.20
M2C	C234C26	40.50	47.00	M2F	C234F26	38.75	44.45
M3C	C234C39	41.32	49.53	M3F	C234F39	40.25	47.87
M4C	C234C52	42.54	50.16	M4F	C234F52	39.25	46.93
M5C	C216C44	38.71	45.27	M5F	C216F44	36.49	44.55
M6C	C216C66	39.86	46.40	M6F	C216F66	38.14	46.21
M7C	C216C88	41.27	48.75	M7F	C216F88	40.06	48.39
M8	<u>C320</u>	47.80	54.87	M8	<u>C320</u>	47.81	54.87
M9C	C288C32	48.62	55.99	M9F	C288F32	46.81	55.02
M10C	C288C48	50.85	57.56	M10F	C288F48	47.93	57.31
M11C	C288C64	50.55	56.95	M11F	C288F64	46.69	54.76
M12C	C266C54	48.26	55.57	M12F	C266F54	45.90	52.33
M13C	C266C81	50.54	57.43	M13F	C266F81	46.23	53.95
M14C	C266C108	51.22	59.84	M14F	C266F108	47.52	55.76
M15	<u>C400</u>	60.53	72.33	M15	<u>C400</u>	60.53	72.33
M16C	C360C40	57.90	68.96	M16F	C360F40	57.76	71.65
M17C	C360C60	60.88	72.88	M17F	C360F60	61.10	75.06
M18C	C360C80	63.26	73.84	M18F	C360F80	63.31	73.42
M19C	C332C68	58.87	68.65	M19F	C332F68	55.27	69.79
M20C	C332C102	60.19	72.06	M20F	C332F102	58.44	71.72
M21C	C332C136	62.91	73.15	M21F	C332F136	61.12	74.94

The quantities of Class F fly ash in the concrete mixtures each did not play a great role in the compressive strength properties. However, the effects of Class F fly ash on the mechanical properties of the concrete did not vary much from the findings of the previous researchers (Papadakis, 1999). Many previous studies have also shown that, at any percentage, the replacement of Portland cement with fly ash in concrete on a one-for-one basis, either by volume or by weight, results in lower compressive strength up to about 3 months of curing, with the development of greater strengths beyond 6 months (Berry, & Malhotra, 1980). Bloem (1954) stated that after a slowing of the early rate of strength contribution by Portland cement, the continued pozzolanic activity of fly ash contributes to increased strength gains at greater ages if the concrete is kept moist. Fraay, Bijen, & De Haan (1989) explained this phenomenon, stating that the glass material in fly ash is broken down only when the pH value of the pore water is at least 13.2, and the increase in the alkalinity of the pore water requires that a certain amount of hydration of the Portland cement in the mix has taken place. Therefore, the pozzolanic reaction of Class F fly ash does not begin until a couple of months. In this study, Class F fly ash specimens were not cured in water to understand after 90 d for compressive strength properties of Class F fly ash. So, the test results indicate until that time period.

Resistance to sulfate attack

Linear expansion and weight loss

Expansion and weight have been monitored in order to understand the main mechanisms of degradation. The results on the effects of magnesium sulfate solution in high concentration and the addition of Class C and Class F fly ashes on the expansion of concrete specimens are shown in Figures 2-4, respectively. Linear expansion values were compared with respect to the Class C and Class F additive specimens had similar compressive strength values to control concretes for each series in which the specimens were immersed. The expansion of the concrete prisms stored in the magnesium sulfate solutions was measured at predetermined times of exposure up to one year. It is clearly evident that the expansion of the control concrete prisms is much larger than those the concretes made with the Class C and Class F fly ashes for each series. The concretes containing Class C and Class F fly ashes showed a “linear” pattern of expansion throughout one-year period in magnesium sulfate solution.

Figure 2. Expansion of concrete prisms exposed to 15 % magnesium sulfate solution for C260 series. Source: Own elaboration.

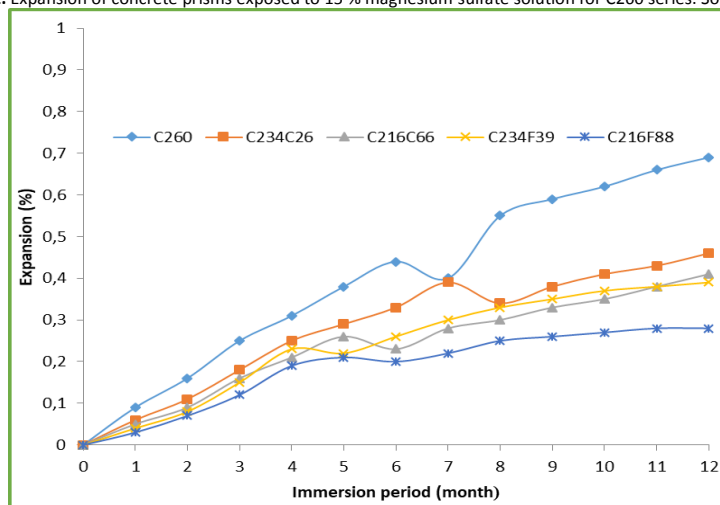


Figure 3. Expansion of concrete prisms exposed to 15% magnesium sulfate solution for C320 series. Source: Own elaboration.

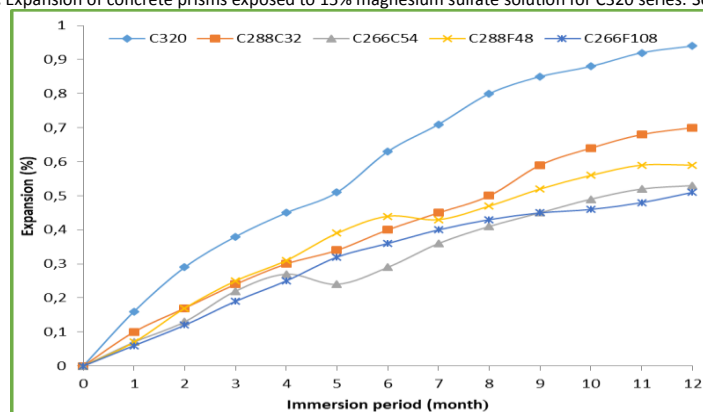


Figure 4. Expansion of concrete prisms exposed to 15 % magnesium sulfate solution for C400 series. Source: Own elaboration.

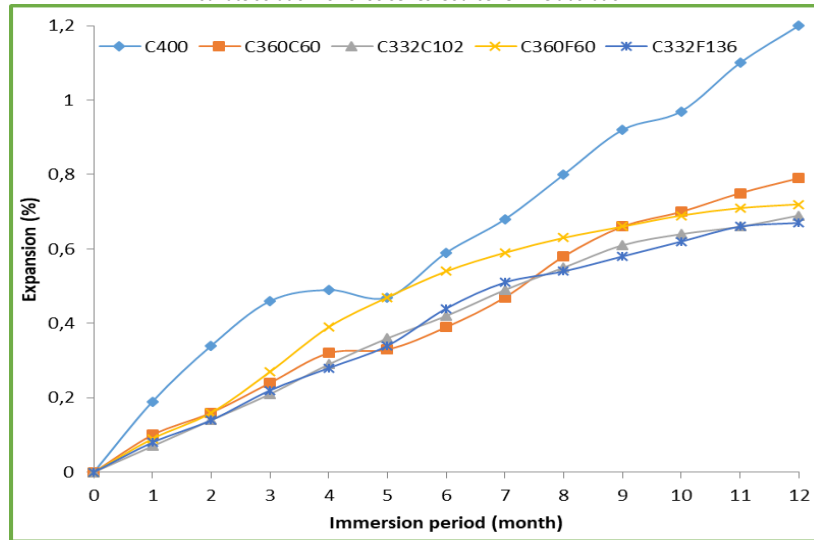
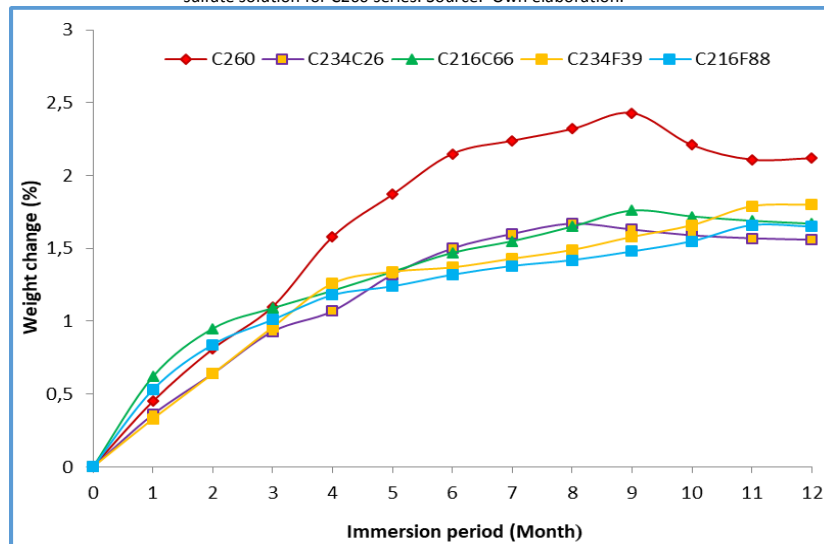


Figure 5. Weight change of concrete prisms exposed to 15 % magnesium sulfate solution for C260 series. Source: Own elaboration.



The expansion values were in the range of 0.03% - 0.69% through one-year immersion period for C260 series. C216F88 mixture had the lowest expansion and the control mixture had the highest one. In terms of expansion, the concretes containing Class C and Class F fly ashes exhibited expansion in the range of 0.06% - 0.92% for C320 series. C266F108 mixture had the lowest expansion and the control mixture also had the highest one. For C400 series, the concretes containing Class C and Class F fly ashes mixtures showed expansion values in the range of 0.07% - 1.2% and the lowest sulfate expansion value was achieved by prism of the concrete extracted from the C332F136 mixture and the highest sulfate expansion value obtained from the control mixture. The test results indicated that in higher level of addition of Class C and Class F fly ashes mixtures, less linear expansion occurred in magnesium sulfate solution for each series. In other words, the higher level of addition of Class C and Class F fly ashes, proved particularly beneficial in terms of expansion. When similar compressive strength values taking into account for each series, Class F type fly ash performed better than Class C type fly ash as expansion. ACI Committee 232 recognizes that the use of low-calcium fly ash should significantly decrease sulfate expansion (ACI Committee 232, 1996). In summary, it was found that the concrete specimens exposed to this high concentration of magnesium sulfate solution showed significant increase in expansion values.

When cement amount was increased it can be seen that the expansion values also increased. Control concretes produce comparatively greater amounts of portlandite ($\text{Ca}(\text{OH})_2$) on hydration than Class C and Class F fly ashes additive concretes. Leaching of portlandite can thus increase ingress of sulfate ions in cement matrix. Moreover, reaction with sulfate is likely to produce more gypsum (CaSO_4) and more ettringite ($\text{C}_3\text{A} \cdot 3\text{CaSO}_4 \cdot 32\text{H}_2\text{O}$), which are responsible for more expansion (Fraay, Bijen, & De Haan, 1989; Rozière, Loukili, El Hachem, & Grondin, 2009).

Essentially, two forms of sulfate attack are known to exist: (1) reaction with alumina-bearing hydration products, and/or unhydrated tricalcium aluminate (C_3A) to produce ettringite; and (2) reaction with calcium hydroxide to produce gypsum. In hardened concrete, the formation of ettringite by sulfate attack can, but does not always, result in expansion. Because of concrete's low tensile strength, expansive strains resulting from ettringite formation during sulfate attack can lead to cracking and reduced performance. Gypsum, in addition to ettringite, can be produced during sulfate attack through cation exchange reactions. Sulfate attack through gypsum formation can result in smaller expansion, but is more generally known to manifest itself through loss of stiffness, strength, and adhesion (Monteiro, & Kurtis, (2003). Previous studies suggest that gypsum formation during sulfate attack is expansive (Tian, & Cohen, 2000; Santhanam, Cohen, & Olek 2002), but ettringite might form afterwards, contributing to expansion.

In addition to the formation of ettringite and gypsum and its subsequent expansion, the deterioration due to sulfate attack is partially caused by the degradation of calcium silicate hydrate (C-S-H) gel through leaching of the calcium compounds. This process leads to loss of C-S-H gel stiffness and overall deterioration of the cement paste matrix (Mehta, 1983). Expansion and cracking are generally attributed to expansive forces generated by sulfate reacting with the calcium aluminium hydrates to form ettringite and loss of weight and strength are generally attributed to reactions where sulfate attacks and breaks down the calcium silicate hydrate (C-S-H), which is the main binding component of hardened cement (Higgins, 2003). In a comprehensive review on the sulfate attack, Bonen and Cohen (1992a) and Bonen, & Cohen (1992b) conducted microstructural analyses on Portland cement paste exposed to magnesium sulfate solution for 1 year. They observed the formation of a "surface double-layer" that was composed of brucite and gypsum layers and a sequential formation of inner layers of gypsum, similar to the occurrence of lisegang bands. Ettringite and monosulfate were only found in minor amounts. Mehta (1993) pointed out that, in most cases, the loss of adhesion and strength, not expansion and cracking, is the primary manifestation of sulfate attack.

The weight loss of various concrete specimens exposed to magnesium sulfate solution with immersion period is presented in Figures 5-7. Every month, the weight of each sample was measured at about 20 °C. There was a continuously mass increase for all the concretes with exposure age. The rate of mass increase of concrete decreases when increasing the replacement level of Class C and Class F fly ashes. So, the least mass increase was found in the mixtures containing higher level of Class C and Class F fly ashes. The weight changes of the specimens were in the range of 0.09% - 0.80% through one-year immersion period for C260 series. For C320 series, the Class C and Class F fly ashes additive concretes showed weight change values in the range of 0.34% - 1.71%. In terms of weight change, the Class C and Class F fly ashes additive concretes exhibited weight change in the range of 0.09% - 0.80% for C400 series. When cement amount was increased it can be seen that the weight change values also decreased and control concretes had higher weight change values compared with the specimens containing Class C and Class F fly ashes for each series. The test results indicated that all the specimens showed mass increase through one-year immersion period. The mass increase is due to swelling caused by gypsum and/or ettringite formation in damaged concrete specimens (Rozière, Loukili, El Hachem, & Grondin, 2009). Furthermore, this phenomenon is attributable to the filling up of pores by the expansive reaction products, thereby densifying the hardened concrete mixtures and increasing the weight (Lee, 2009). Additionally, the general increase of weight was the result of continuous water absorption, slowly compensating for the chemical shrinkage due to the hydration of the cement (Persson, 2003). So, it is obvious that the use of weight change to predict the sulfate resistance is not an accurate method.

Figure 6. Weight change of concrete prisms exposed to 15 % magnesium sulfate solution for C320 series. Source: Own elaboration.

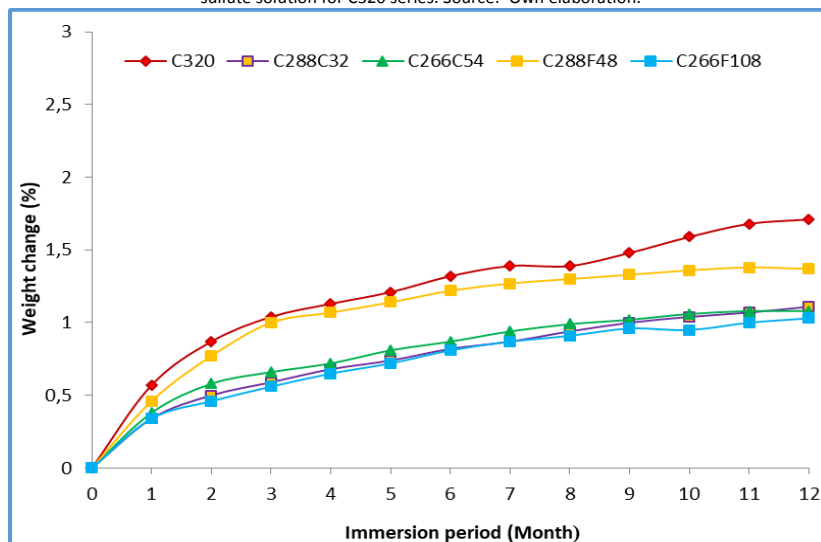
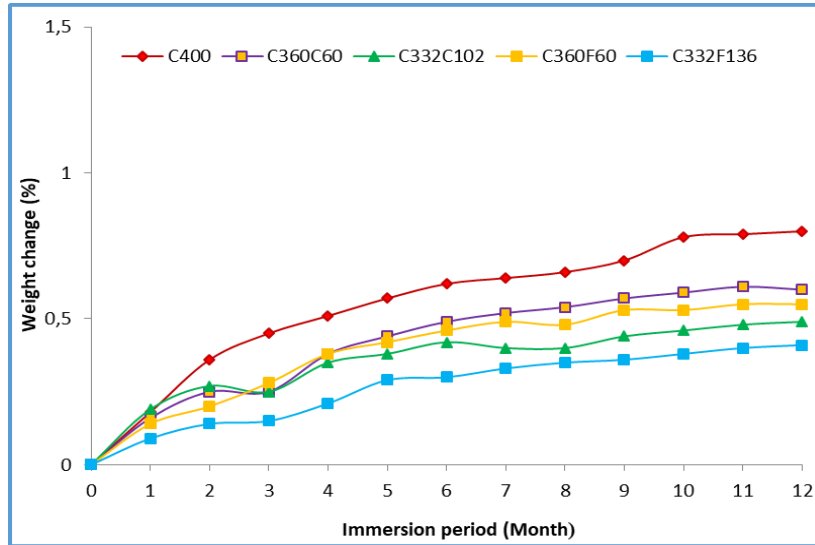


Figure 7. Weight change of concrete prisms exposed to 15 % magnesium sulfate solution for C400 series. Source: Own elaboration



Artificial neural network model for prediction of experimental results

ANN can exhibit a surprising number of human brain characteristics (Öztaş, Pala, Özbay, Kanca, Caglar, & Bhatti, 2006; Demir, Topçu, & Kuşan, 2011). The fundamental concept of neural networks is the structure of the information processing system (Adhikary, & Mutsuyoshi, 2004; Saridemir, 2009). They are consisting of a large number of simple processing elements called as neurons. The neurons are used in ANN. These neurons are connected with connection link. Each link has a weight that is multiplied by transmitted signal in network. Each neuron has an activation function to determine the output. There are many kinds of activation functions. Usually nonlinear activation functions such as sigmoid, step are used. ANNs are trained by experience, when an unknown input is applied to the network it can generalize from past experiences and produce a new result (Hanbay, Turkoglu, & Demir, 2008a; Haykin, 1994; Hanbay, Turkoglu, & Demir, 2008b; Bilim, Atiş, & Tanyildizi, Karahan, 2009).

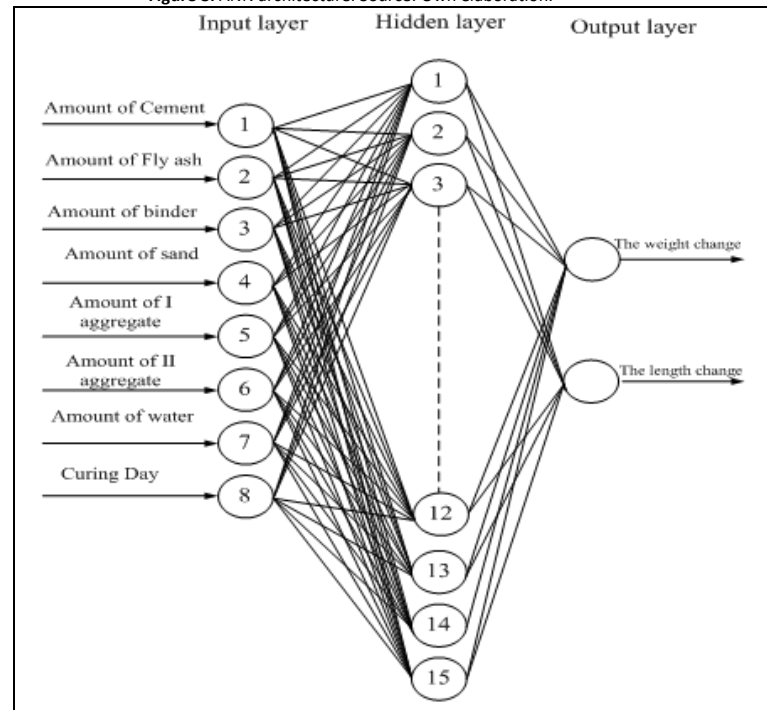
$$u = \sum_{j=0}^m x_j w_j - b \text{ and } V = f(u) \quad (1)$$

Artificial neural networks are systems that are deliberately tended to make use of some organizational principles resembling those of the human brain (Hanbay, Turkoglu, & Demir, 2008a; Haykin, 1994; Hanbay, Turkoglu, & Demir, 2008b; Bilim, Atiş, & Tanyildizi, Karahan, 2009). They represent the promising new generation of information processing systems.

When designing an ANN model, a number of considerations must be taken into account. At first the suitable structure of the ANN model must be chosen. Then, the activation function needs to be determined. The number of layers and the number of units in each layer must be chosen. Generally desired model consists of a number of layers. The most general model assumes complete interconnections between all units. These connections can be bidirectional or unidirectional. ANN can create its own organization or representation of the information it receives during learning time (Hanbay, Turkoglu, & Demir, 2008a; Haykin, 1994; Hanbay, Turkoglu, & Demir, 2008b; Bilim, Atiş, & Tanyildizi, Karahan, 2009).

In this study, the problem is proposed to network models by means of eight input and two output parameters. The parameters such as amount of cement, amount of fly ash, amount of binder, amount of sand, amount of type I aggregate, amount of type II aggregate, amount of water, curing period were selected as input variables. The model output variables were the weight and length changes of the concrete exposed to sulfate. Data sets including 180 data samples obtained from experimental studies were used for artificial neural networks. The data were normalized by dividing with max values. ANN architecture used for this study is given in Figure 8.

Figure 8. ANN architecture. Source: Own elaboration.



The all algorithms of ANN were used for this study but the BFGS quasi-Newton backpropagation, Fletcher-Powell conjugate gradient backpropagation, Polak-Ribiere conjugate gradient backpropagation, Gradient descent with adaptive lr backpropagation, Gradient descent w/momentum & adaptive lr backpropagation, Levenberg-Marquardt backpropagation, One step secant backpropagation, Random order incremental training w/learning functions, Scaled conjugate gradient backpropagation were just learning. The computer program was performed under MATLAB software using the neural network toolbox. In the training, the number of neuron on the hidden layer changed to find best results. The best result for BFGS quasi-Newton backpropagation algorithm was obtained from the fifteen neurons. The best result for Fletcher-Powell conjugate gradient backpropagation was obtained from the fourteen neurons. The best result for Polak-Ribiere conjugate gradient backpropagation was obtained from the sixteen neurons. The best result for Gradient descent with adaptive lr backpropagation was obtained from the eighteen neurons. The best result for Gradient descent w/momentum & adaptive lr backpropagation was obtained from the eighteen neurons. The best result for Levenberg-Marquardt backpropagation was obtained from the six neurons. The best result for One step secant backpropagation was obtained from the sixteen neurons. The best result for Random order incremental training w/learning functions was obtained from the sixteen neurons. The best result for Scaled conjugate gradient backpropagation was obtained from the nine neurons. A data set including 180 data samples obtained from experimental studies were used for artificial neural networks. From these, 90 data patterns were used for training the network, and the remaining 90 patterns were randomly selected and used as the test data set. Figure 9 and Figure 10 present the measured values versus predicted values by ANN model with R^2 coefficients. Figure 9 and Figure 10 show that the best algorithm for length changes of concrete exposed to sulfate is BFGS quasi-Newton backpropagation algorithm with R^2 of 0.9804 while the best algorithm for weight changes of concrete exposed to sulfate is the Levenberg-Marquardt backpropagation algorithm with R^2 of 0.9746. The best results using the Levenberg-Marquardt backpropagation algorithm in this study are similar to Karahan et al. (2008). The training performance during the training process is given in Figure 11 where the variation of mean-square error with training epochs is illustrated.

Figure 9. Linear relationship between the measured and predicted length changes; a) the BFGS quasi-Newton backpropagation algorithm, b) the Fletcher-Powell conjugate gradient backpropagation algorithm, c) the Polak-Ribiere conjugate gradient backpropagation algorithm, d) the Gradient descent with adaptive lr backpropagation algorithm, e) the Gradient descent w/momentum & adaptive lr backpropagation algorithm, f) the Levenberg-Marquardt backpropagation algorithm, g) the One step secant backpropagation algorithm, h) the Random order incremental training w/learning functions algorithm, i) the Scaled conjugate gradient backpropagation algorithm. Source: Own elaboration.

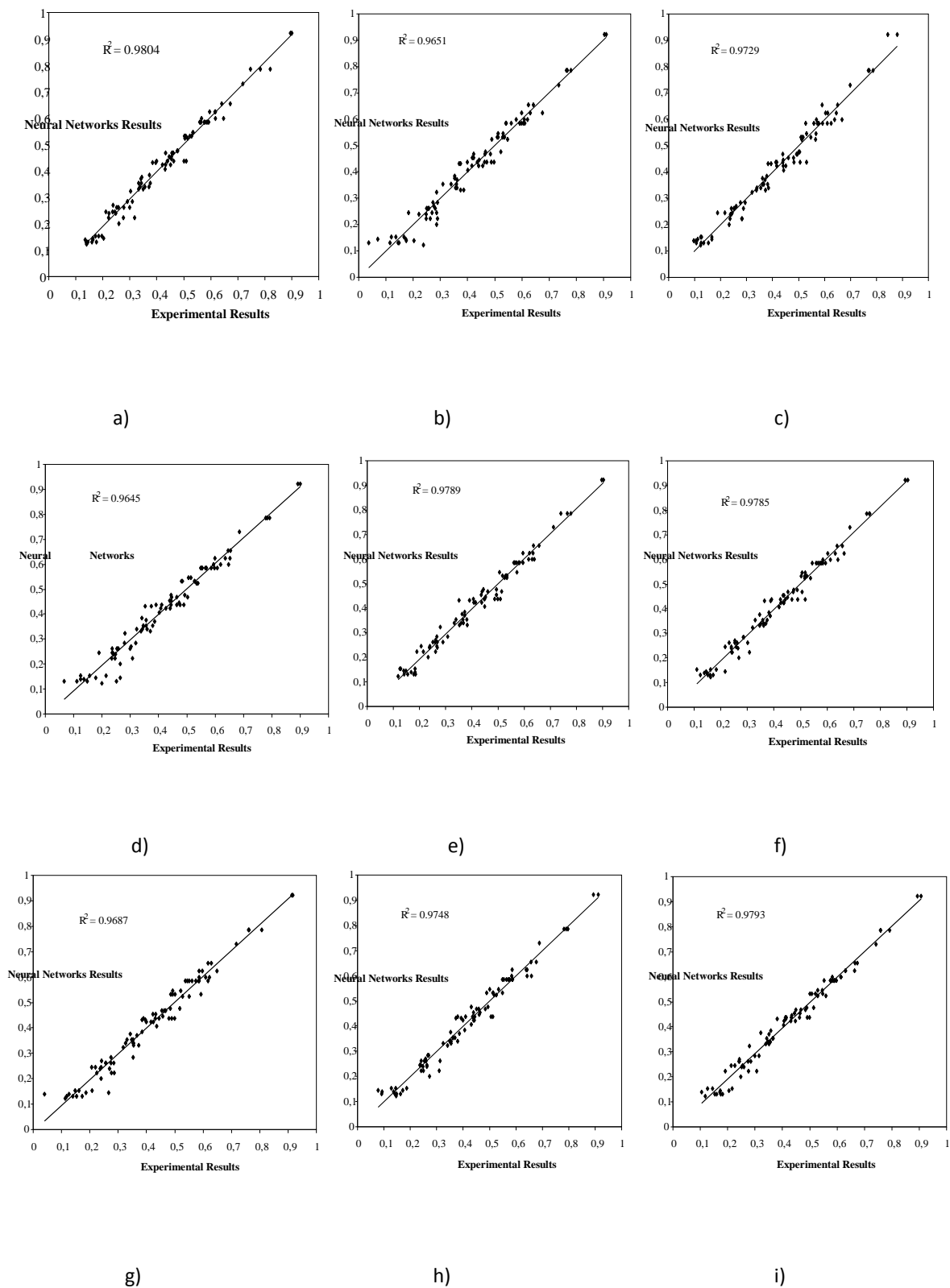


Figure 10. Linear relationship between the measured and predicted weight changes; a) for the BFGS quasi-Newton backpropagation algorithm, b) the Fletcher-Powell conjugate gradient backpropagation algorithm, c) the Polak-Ribiere conjugate gradient backpropagation algorithm, d) the Gradient descent with adaptive lr backpropagation algorithm, e) the Gradient descent w/momentum & adaptive lr backpropagation algorithm, f) the Levenberg-Marquardt backpropagation algorithm, g) the One step secant backpropagation algorithm, h) the Random order incremental training w/learning functions algorithm, i) the Scaled conjugate gradient backpropagation algorithm. Source: Own elaboration.

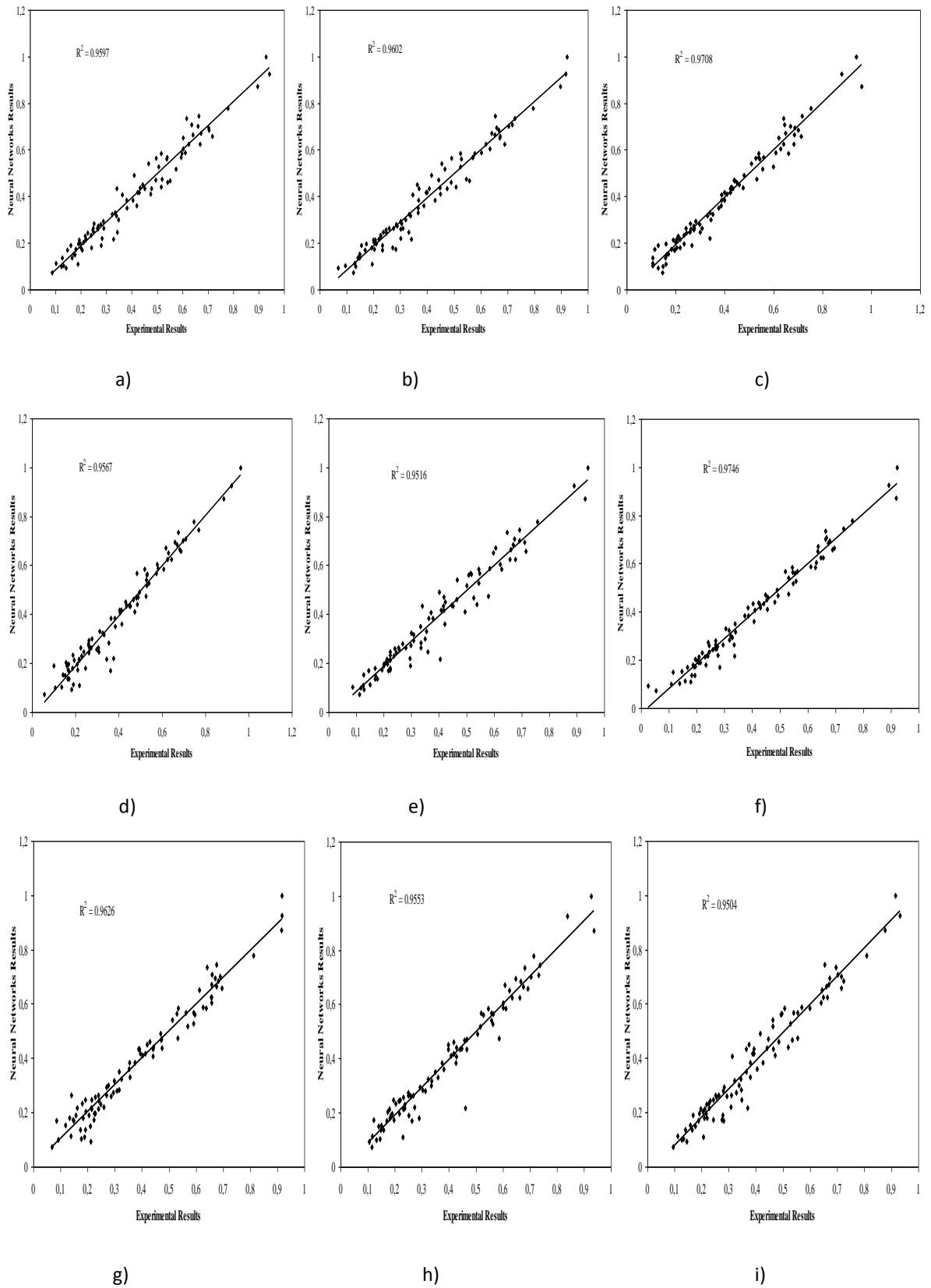
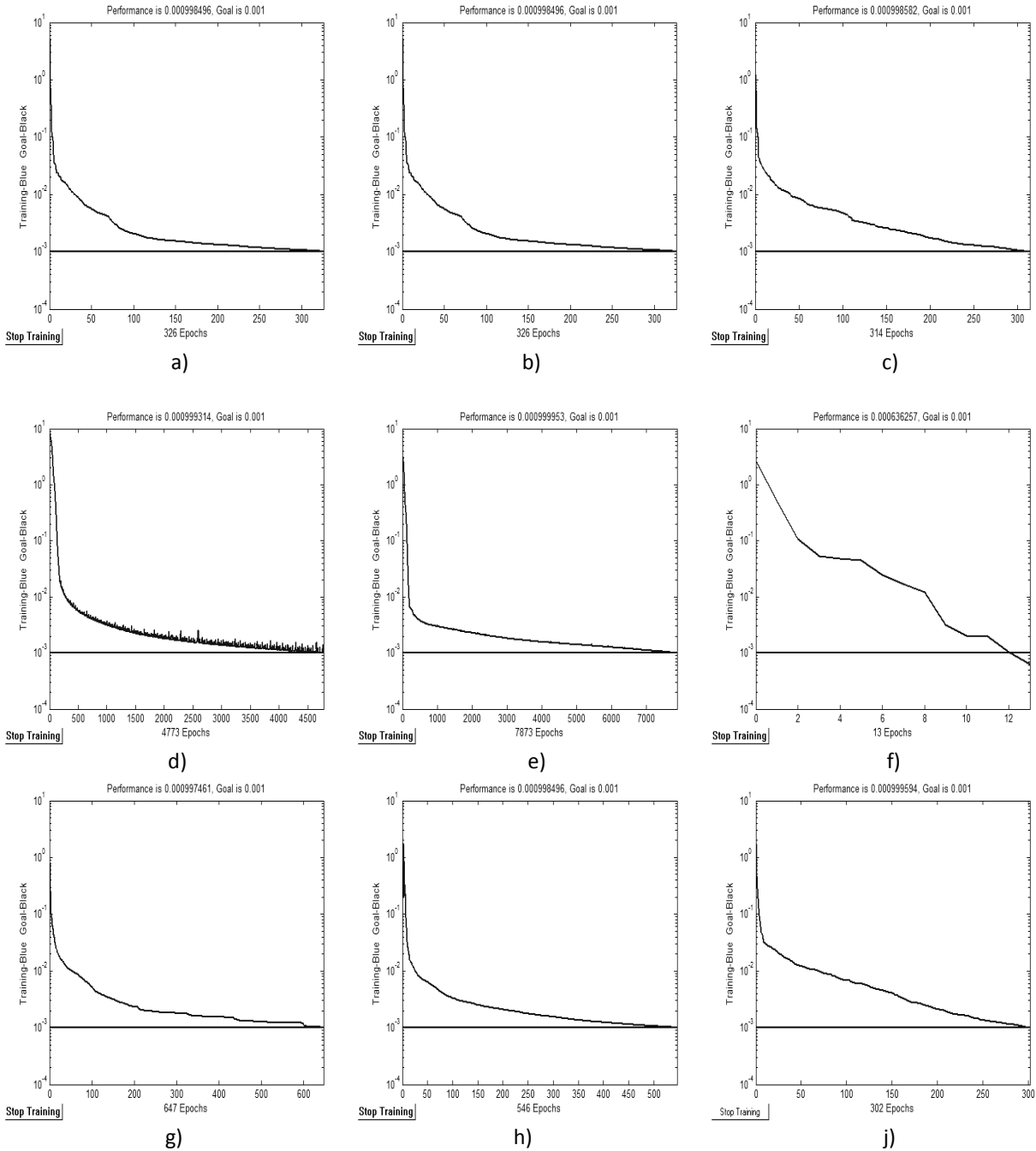


Figure 11. Training performance **a)** BFGS quasi-Newton backpropagation algorithm, **b)** Fletcher-Powell conjugate gradient backpropagation algorithm, **c)** the Polak-Ribiere conjugate gradient backpropagation algorithm, **d)** the Gradient descent with adaptive lr backpropagation algorithm, **e)** Gradient descent w/momentum & adaptive lr backpropagation algorithm, **f)** Levenberg-Marquardt backpropagation algorithm, **g)** One step secant backpropagation algorithm, **h)** Random order incremental training w/learning functions algorithm, **j)** Scaled conjugate gradient backpropagation algorithm. Source: Own elaboration.



Conclusions

Laboratory tests were performed to determine the deterioration induced by the magnesium sulfate on the control and Class C and Class F type fly ashes additive concretes. The results of the tests are as follows:

- The use of Class C type fly ash instead of Class F type fly ash with the same cement dosage and fly ash percentage generally caused to higher compressive strength.
- The expansion values were in the range of % 0.03 - % 1.2 through one-year immersion period for C260, C320 and C400 series. The test results indicated that in higher level addition of Class C and Class F fly ashes mixtures, less linear expansion occurred in magnesium sulfate solution for each series. When cement amount was increased, the weight change values also decreased and control concretes had higher weight change values compared with the specimens containing Class C and Class F fly ashes for each series. All the specimens showed mass increase through one-year immersion period.

- Experimental results showed that ANN has been used for the prediction of length changes of concrete exposed to sulfate. The neural networks-based model gave high prediction accuracy and correlation. The best algorithm for length changes of concrete exposed to sulfate is BFGS quasi-Newton backpropagation algorithm with R^2 of 0.9804 while the best algorithm for weight changes of concrete exposed to sulfate is the Levenberg-Marquardt backpropagation algorithm with R^2 of 0.9746. Therefore, it is possible to predict length changes of concrete exposed to sulfate using artificial neural networks.

References

- ACI Committee 232. (1996). Use of Fly Ash in Concrete (232.2R-96), American Concrete Institute, Farmington Hills, MI, USA.
- Adhikary, B. B., & Mutsuyoshi, H. (2004). Artificial neural networks for the prediction of shear capacity of steel plate strengthened RC beams. *Construction and Building Materials*, 18(6), 409-417.
- Al-Akhras, N. M. (2006). Durability of metakaolin concrete to sulfate attack. *Cement and Concrete Research*, 36(9), 1727-1734.
- Alonso, J.L., & Wesche, K. (1991). Characterization of fly ash. In: Wesche K, editor. Fly ash in concrete. London: Taylor and Francis, p. 3–23.
- ASTM C 1012. (2002). Standard Test Method for Length Change of Hydraulic cement Mortar Exposed to a Sulfate Solution. American Society for Testing and Materials. Philadelphia.
- Atiş, C. D., & Karahan, O. (2009). Properties of steel fiber reinforced fly ash concrete. *Construction and Building Materials*, 23(1), 392-399.
- Aydin, S., Yiğiter, H., & Baradan, B. (2005). Effect of steam curing on class C high-volume fly ash concrete mixtures. *Cement and Concrete Research*, 35(6), 1122-1127.
- Berry, E. E., & Malhotra, V. M. (1980, March). Fly ash for use in concrete—a critical review. *In Journal Proceedings* (Vol. 77, No. 2, pp. 59-73).
- Bilim, C., Atiş, C. D., & Tanyildizi, H., Karahan, O. (2009). Predicting the compressive strength of ground granulated blast furnace slag concrete using artificial neural network. *Advances in Engineering Software*, 40(5), 334-340.
- Bloem D.L. (1954). Effect of curing conditions on compressive strength of concrete test specimens, NSGA Circular No. 59 and NRMC Publication No. 53, National Ready Mixed Concrete Association: Silver Spring; December.
- Bonen, D., & Cohen, M.D. (1992a). Magnesium sulfate attack on Portland cement paste-I. Microstructural analysis, *Cement and Concrete Research*, 22, 169-180.
- Bonen, D., & Cohen, M.D. (1992b). Magnesium sulfate attack on Portland cement paste-II. Chemical and mineralogical analysis, *Cement and Concrete Research*, 22, 707-718.
- Cao, C., Sun, W., & Qin, H. (2000). The analysis on strength and fly ash effect of roller-compacted concrete with high volume fly ash. *Cement and Concrete Research*, 30(1), 71-75.
- Chatterji, S. (1995). On the applicability of Fick's second law to chloride ion migration through Portland cement concrete. *Cement and Concrete Research*, 25(2), 299-303.
- Chung, C. W., Shon, C. S., & Kim, Y. S. (2010). Chloride ion diffusivity of fly ash and silica fume concretes exposed to freeze–thaw cycles. *Construction and Building Materials*, 24(9), 1739-1745.
- Demir, A., Topçu, İ. B., & Kuşan, H. (2011). Modeling of some properties of the crushed tile concretes exposed to elevated temperatures. *Construction and Building Materials*, 25(4), 1883-1889.
- Felekoglu, B. (2006). Utilisation of Turkish fly ashes in cost effective HVFA concrete production. *Fuel*, 85(12-13), 1944-1949.
- Fraay, A. L. A., Bijen, J. M., & De Haan, Y. M. (1989). The reaction of fly ash in concrete a critical examination. *Cement and Concrete Research*, 19(2), 235-246.
- Girardi, F., Vaona, W., & Di Maggio, R. (2010). Resistance of different types of concretes to cyclic sulfuric acid and sodium sulfate attack. *Cement and Concrete Composites*, 32(8), 595-602.
- Goktepe, A. B., Inan, G., Ramyar, K., & Sezer, A. (2006). Estimation of sulfate expansion level of PC mortar using statistical and neural approaches. *Construction and Building Materials*, 20(7), 441-449.
- Hale, W. M., Freyre, S. F., Bush Jr, T. D., & Russell, B. W. (2008). Properties of concrete mixtures containing slag cement and fly ash for use in transportation structures. *Construction and Building Materials*, 22(9), 1990-2000.
- Hanbay, D., Turkoglu, I., & Demir, Y. (2008a). An expert system based on wavelet decomposition and neural network for modeling Chua's circuit. *Expert Systems with Applications*, 34, 2278-2283.
- Hanbay, D., Türkoğlu, I., & Demir, Y. (2008b). An Expert System Based on Wavelet Decomposition and Neural Network for Modeling Chua's Circuit. *Expert systems with applications*, 34(4), 2278-2283.
- Haykin, S. (1994). Neural networks, a comprehensive foundation, College Publishing Comp. Inc.
- Hekal, E. E., Kishar, E., & Mostafa, H. (2002). Magnesium sulfate attack on hardened blended cement pastes under different circumstances. *Cement and Concrete Research*, 32(9), 1421-1427.

- Higgins, D. D. (2003). Increased sulfate resistance of ggbs concrete in the presence of carbonate. *Cement and Concrete Composites*, 25(8), 913-919.
- Hooton, R. D. (1993). Influence of silica fume replacement of cement on physical properties and resistance to sulfate attack, freezing and thawing, and alkali-silica reactivity. *Materials Journal*, 90(2), 143-151.
- Inan, G., Göktepe, A. B., Ramyar, K., & Sezer, A. (2007). Prediction of sulfate expansion of PC mortar using adaptive neuro-fuzzy methodology. *Building and Environment*, 42(3), 1264-1269.
- Jain, J. A., & Neithalath, N. (2010). Chloride transport in fly ash and glass powder modified concretes—influence of test methods on microstructure. *Cement and Concrete Composites*, 32(2), 148-156.
- Karahan, O., Tanyildizi, H., & Atis, C. D. (2008). An artificial neural network approach for prediction of long-term strength properties of steel fiber reinforced concrete containing fly ash. *Journal of Zhejiang University-SCIENCE A*, 9(11), 1514-1523.
- Lai, S., & Serra, M. (1997). Concrete strength prediction by means of neural network. *Construction and Building Materials*, 11(2), 93-98.
- Lee, S. C. (2003). Prediction of concrete strength using artificial neural networks. *Engineering Structures*, 25(7), 849-857.
- Lee, S. T. (2009). Influence of recycled fine aggregates on the resistance of mortars to magnesium sulfate attack. *Waste Management*, 29(8), 2385-2391.
- Li, G., & Zhao, X. (2003). Properties of concrete incorporating fly ash and ground granulated blast-furnace slag. *Cement and Concrete Composites*, 25(3), 293-299.
- Liu, M. (2010). Self-compacting concrete with different levels of pulverized fuel ash. *Construction and Building Materials*, 24(7), 1245-1252.
- Malhotra, V. M., Zhang, M. H., Read, P. H., & Ryell, J. (2000). Long-term mechanical properties and durability characteristics of high-strength/high-performance concrete incorporating supplementary cementing materials under outdoor exposure conditions. *Materials Journal*, 97(5), 518-525.
- Mehta, P. K. (1983). Mechanism of sulfate attack on portland cement concrete—Another look. *Cement and Concrete Research*, 13(3), 401-406.
- Mehta, P.K. (1993). Sulfate attack on concrete: A critical review, in: R.R. Villarreal (Ed.), *Concrete Durability*, Univ. Autonoma de Nuevo Leon, 107-132.
- Mehta, PK, & Monteiro, P.J.M. (1993). *Concrete structure, properties, and materials*. 2nded. NJ: Prentice Hall; p. 209-214.
- Melo, K. A., & Carneiro, A. M. (2010). Effect of Metakaolin's finesses and content in self-consolidating concrete. *Construction and Building Materials*, 24(8), 1529-1535.
- Mohammed, B. S., & Fang, O. C. (2011). Mechanical and durability properties of concretes containing paper-mill residuals and fly ash. *Construction and Building Materials*, 25(2), 717-725.
- Monteiro, P. J., & Kurtis, K. E. (2003). Time to failure for concrete exposed to severe sulfate attack. *Cement and Concrete Research*, 33(7), 987-993.
- Ni, H. G., & Wang, J. Z. (2000). Prediction of compressive strength of concrete by neural networks. *Cement and Concrete Research*, 30(8), 1245-1250.
- Nochaiya, T., Wongkeo, W., & Chaipanich, A. (2010). Utilization of fly ash with silica fume and properties of Portland cement–fly ash–silica fume concrete. *Fuel*, 89(3), 768-774.
- Öztaş, A., Pala, M., Özbay, E., Kanca, E., Caglar, N., & Bhatti, M. A. (2006). Predicting the compressive strength and slump of high strength concrete using neural network. *Construction and Building Materials*, 20(9), 769-775.
- Papadakis, V. G. (1999). Effect of fly ash on Portland cement systems: Part I. Low-calcium fly ash. *Cement and Concrete Research*, 29(11), 1727-1736.
- Persson, B. (2003). Sulphate resistance of self-compacting concrete. *Cement and Concrete Research*, 33:1933–1938.
- Roy, S. K., Chye, L. K., & Northwood, D. O. (1993). Chloride ingress in concrete as measured by field exposure tests in the atmospheric, tidal and submerged zones of a tropical marine environment. *Cement and Concrete Research*, 23(6), 1289-1306.
- Rozière, E., Loukili, A., El Hachem, R., & Grondin, F. (2009). Durability of concrete exposed to leaching and external sulphate attacks. *Cement and Concrete Research*, 39(12), 1188-1198.
- Santhanam, M., Cohen, M.D., & Olek J. (2002). Modeling the effects of solution temperature and concentration during sulfate attack on cement mortars. *Cement and Concrete Research*, 32, 585–92.
- Saridemir, M. (2009). Predicting the compressive strength of mortars containing metakaolin by artificial neural networks and fuzzy logic. *Advances in Engineering Software*, 40(9), 920-927.
- Siddique, R. (2011). Properties of self-compacting concrete containing class F fly ash. *Materials & Design*, 32(3), 1501-1507.
- Sorrentino, D., Lacroix, M., Gines, S., & Chabanis, F. (1994). Behavior of a wide series of mortar bars (20 to 120 MPa) stored in MgSO₄ or in sea-water solutions, in: W. Kurdowski (Ed.), *Corrosion of Cement Paste*, Polish Ceramic Society, 13– 32.
- Tanyildizi, H. (2016). The investigation of microstructure and strength properties of lightweight mortar containing mineral admixtures exposed to sulfate attack. *Measurement*, 77, 143-154.
- Tanyildizi, H. (2017). Prediction of compressive strength of lightweight mortar exposed to sulfate attack. *Computers and Concrete*, 19(2), 217-226.

- Tanyildizi, H. (2018). Long-term performance of the healed mortar with polymer containing phosphazene after exposed to sulfate attack. *Construction and Building Materials*, 167, 473-481.
- Tian, B., & Cohen, M. D. (2000). Does gypsum formation during sulfate attack on concrete lead to expansion?. *Cement and Concrete Research*, 30(1), 117-123.
- Topcu, I. B., & Canbaz, M. (2007). Effect of different fibers on the mechanical properties of concrete containing fly ash. *Construction and Building Materials*, 21(7), 1486-1491.
- Torii, K., & Kawamura, M. (1994). Effects of fly ash and silica fume on the resistance of mortar to sulfuric acid and sulfate attack. *Cement and Concrete Research*, 24(2), 361-370.
- Trtnik, G., Kavčič, F., & Turk, G. (2009). Prediction of concrete strength using ultrasonic pulse velocity and artificial neural networks. *Ultrasonics*, 49(1), 53-60.
- Yen, T., Hsu, T. H., Liu, Y. W., & Chen, S. H. (2007). Influence of class F fly ash on the abrasion-erosion resistance of high-strength concrete. *Construction and Building Materials*, 21(2), 458-463.